

THERMAL CHARACTERIZATION OF MULTI-WALL CARBON NANOTUBE BUNDLES BASED ON PULSED LASER-ASSISTED THERMAL RELAXATION

JIAQI GUO

*Department of Mechanical Engineering
N104 Walter Scott Engineering Center
University of Nebraska-Lincoln
Lincoln, NE 68588-0656, USA
jjguoffc@bigred.unl.edu*

XINWEI WANG*

*Department of Mechanical Engineering
3027 H.M. Black Engineering Building
Iowa State University, Ames, IA 50011-2161, USA
xwang3@iastate.edu*

DAVID B. GEOHEGAN and GYULA ERES

*Materials Science and Technology Division &
Center for Nanophase Materials Sciences
Oak Ridge National Laboratory
1 Bethel Valley Road, MS-6056
Oak Ridge, TN 37831-6056, USA*

Received 16 January 2008

Revised 1 February 2008

A novel transient technique is developed to measure the thermal diffusivity of one-dimensional microscale wires. In this technique, a pulsed nanosecond laser is used to quickly heat the wire. After laser heating, the wire temperature decays slowly. Such temperature decay is sensed and used to determine the thermal diffusivity of the wire. A 25.4 μm thin Pt wire is characterized to verify this technique. The thermal diffusivity of multi-wall carbon nanotube bundles is measured. Based on the measurement result and the inside structure, the thermal diffusivity of individual carbon nanotubes is estimated.

Keywords: Thermal diffusivity; characterization; nanosecond laser; carbon nanotube.

1. Introduction

One-dimensional micro/nanoscale functional materials have attracted growing interest and are expected to find broader applications in areas like

mechanical strength enhancement, novel chemical and optical sensing, as well as thermal-electrical and chemical-electrical energy conversion. Among these 1D structures, the carbon nanotube is

*Corresponding author.

the most popular, due to its highly efficient conducting of current and heat, remarkable mechanical strength, and even working as the carrier of electron spins. Knowledge of thermal transport in these micro/nanoscale structures is becoming indispensable for future applications since the temperature and thermal response of materials strongly affect their mechanical, optical, and electrical properties. Characterization of the thermophysical properties of micro/nanoscale 1D structures is very challenging due to the great difficulty faced in extremely localized heating and thermal sensing. A large number of experimental, theoretical, and numerical techniques have been developed to characterize the thermophysical properties of micro/nanoscale wires/tubes, like the 3ω method,¹⁻³ the microfabricated device method,^{4,5} molecular dynamics simulation,⁶ and theoretical estimation.⁷ Recent studies in our group have led to the development of novel techniques for measuring the thermophysical properties of individual 1D micro/nanoscale structures. To date, an optical heating and electrical thermal sensing (OHETS) technique,⁸⁻¹⁰ transient electrothermal (TET) technique,^{11,12} and transient photo-electrothermal (TPET) technique¹³ have been developed to measure the thermophysical properties of wires/tubes at micro/nanoscales. The OHETS technique requires relatively long measurement time (usually several hours) and suffers from low signal level (μV), which is also encountered in the 3ω method.¹⁻³ For the other two transient techniques, TET and TPET, limited by the slow rising time of the thermal excitation source ($\sim 2\ \mu\text{s}$ for current in TET¹² and $\sim 10\ \mu\text{s}$ for the laser in TPET¹³), both techniques make it difficult to measure short wires with relatively high thermal diffusivity. For such samples, the time of heat transfer taken to reach the steady state will be short and comparable to the rising time of the electrical current/laser beam, thereby making the experiment difficult to conduct.

In this paper, a pulsed laser-assisted thermal relaxation (PLTR) technique is developed to overcome the drawbacks of the OHETS, TET and TPET techniques while providing comparable fast conducting of experiments and high signal/noise ratio. To test this new technique, thermal diffusivity measurement of platinum (Pt) wire is conducted first. By applying this technique, the thermal diffusivities of two types of multi-wall carbon nanotube (MWCNT) bundles are measured.

2. Theoretical Developments of the Technique

2.1. *Experimental principle*

In the PLTR technique, the to-be-measured wire is suspended over two copper electrodes. Silver paste is placed at the wire/electrode contacts to enhance the mechanical and electrical connection. When running the experiment, a nanosecond laser pulse is used to irradiate the sample wire uniformly to induce a sudden temperature increase. Right after the pulsed heating, the temperature of the wire will gradually go down. Such temperature relaxation is strongly determined by the sample's thermal diffusivity and length. For instance, for a given length, if the wire has a larger thermal diffusivity, it will take shorter time for the temperature to go down and reach its steady state. From this temperature relaxation history, the thermal diffusivity of the wire can be determined. In order to probe its temperature evolution, a small DC current is fed through the wire for the reason that the temperature change will correspondingly lead to a resistance change. As a result, the voltage over the wire will change and will be recorded and used to extract the thermal diffusivity of the wire.

2.2. *Physical model development*

In our experiment, the length of the wire is significantly greater than its diameter, which will simplify the heat transfer mode to one dimensional (in the axial direction of the wire). In the 1D heat transfer equation, the thermal energy generation term is $\dot{q} = \dot{q}_1 + \dot{q}_2$, where \dot{q}_1 is the DC current heating and \dot{q}_2 the laser pulse heating. Since we are only interested in the temperature evolution caused by the pulsed laser heating, its governing equation can be described as:

$$\frac{\partial(\rho c_p T_2)}{\partial t} = k \frac{\partial^2 T_2}{\partial x^2} + \dot{q}_2, \quad (1)$$

with homogeneous boundary conditions and initial conditions, $T_2(x = 0, t) = T_2(x = L, t) = 0$ and $T_2(x, t = 0) = 0$. Here T_2 only represents the temperature variation induced by the pulsed laser heating. The pulsed laser heating source can be simplified as

$$\dot{q}_2 = \begin{cases} q, & 0 \leq t \leq \Delta t, \\ 0, & t > \Delta t. \end{cases} \quad (2)$$

Here Δt is the laser pulse width, and we assume the laser intensity is constant during Δt . Since the

laser heating time ($\sim 10^{-9}$ s) is significantly smaller than the characteristic time of heat transfer in the sample, the above assumption will have a negligible effect on the accuracy of the solution. The solution to the partial differential equation described by Eq. (1) can be obtained from the integral of the Green's function. The average temperature of the wire $T_2(t)$ for the time t larger than Δt is

$$T_2(t) = \frac{8qL^2}{k\pi^4} \sum_{m=1}^{\infty} \frac{\exp[-(2m-1)^2\pi^2\alpha t/L^2]}{(2m-1)^4} \times \{\exp[(2m-1)^2\pi^2\alpha\Delta t/L^2] - 1\}. \quad (3)$$

After normalizing as $T_2^* = [T_2(t) - T_{2,\min}]/(T_{2,\max} - T_{2,\min})$, ($T_{2,\min}$ is 0 and $T_{2,\max}$ is the maximum temperature rise of the sample calculated as $q\Delta t/\rho c_p$), the normalized temperature relaxation simplified using Taylor expansions can be written as

$$T_2^* = \frac{8}{\pi^2} \sum_{m=1}^{\infty} \frac{\exp[-(2m-1)^2\pi^2\alpha t/L^2]}{(2m-1)^2}. \quad (4)$$

Equation (4) shows that for any kind of material of arbitrary length, the normalized temperature relaxation follows the same shape with respect to the Fourier number $\text{Fo}(= \alpha t/L^2)$.

2.3. Methods to determine the thermal diffusivity

Figure 1 shows a typical normalized temperature relaxation curve as an example to discuss the two data analysis methods for determining the sample's thermal diffusivity. The first method is based on a characteristic point on the temperature relaxation curve. It is seen from Eq. (4) that the normalized temperature is only a function of the Fourier number $\text{Fo} = \alpha t/L^2$. Therefore, one single point on the

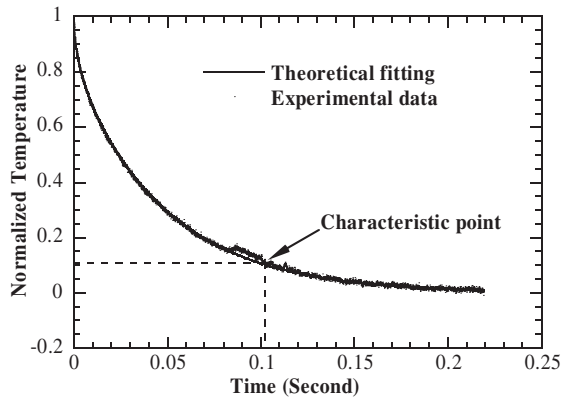


Fig. 1. The normalized temperature versus the theoretical fitting for the Pt wire using both data analysis methods.

T_2^*-t curve can be used to determine the thermal diffusivity of the wire directly. The best characteristic point should have the property that both the y -axis (normalized temperature) and x -axis (time) have very high sensitivity to a small change in $\Delta\alpha$. That is to say, we need the product of ΔT_2^* and Δt to have a maximum value when the thermal diffusivity changes by $\Delta\alpha$, where $\Delta T_2^* = \partial T_2^*/\partial\alpha \cdot \Delta\alpha$ and $\Delta t = \partial t/\partial\alpha \cdot \Delta\alpha$. In order to get the maximum sensitivity, the term $\partial T_2^*/\partial\alpha \cdot \partial t/\partial\alpha$ should reach its maximum value. It is not difficult to find that $\partial T_2^*/\partial\alpha \cdot \partial t/\partial\alpha = \partial T_2^*/\partial\text{Fo} \cdot L^2 \cdot \text{Fo}^2/\alpha^3$.

Using numerical methods and Eq. (4), we find the best characteristic point corresponds to the normalized temperature T_2^* of 0.1097. The corresponding Fourier number is 0.2026, as shown in Fig. 1. When using the characteristic point method, once the characteristic time (Δt_c) is identified from the T_2^*-t curve when the normalized temperature goes down to 0.1097, the thermal diffusivity of the sample can be calculated as $\alpha = 0.2026 \times L^2/\Delta t_c$. In order to better determine the characteristic point from the obtained experimental data, a small set of data points around the characteristic point is used with linear fitting to determine the characteristic point.

The second method to determine the thermal diffusivity of the sample is based on global data fitting of the temperature relaxation curve. In this method, the normalized temperature decrease is calculated using Eq. (4) by using different trial values of thermal diffusivity. The trial value giving the best fit (least square) of the experimental data is taken as the sample's thermal diffusivity.

It needs to be pointed out that the solution developed above is not dependent on the inside structure of the wires/tubes. The only assumption is that the heat diffusion equation can still be applied to the sample in the axial direction. When the sample length is small (comparable to the phonon mean free path), the ballistic feature of heat transfer will become more important. In such a situation, the thermal diffusivity determined using Eq. (4) represents an effective value describing the heat transfer capability of the sample.

3. Experimental Details and Results

3.1. Experimental setup and calibration

In the experiment, a current source (KEITHLEY 6221) is used to provide a constant DC current

through the sample. An Nd:YAG laser operated in periodical pulse mode is used to heat the sample. The pulse width of the laser (7 ns) is much shorter than the characteristic time Δt_c for the measured samples. A high speed digital oscilloscope (TDS7054) with a proper offset is used to capture the fine change of the voltage over the sample. In order to minimize the influence of air convection, the wire is housed in a vacuum at 1×10^{-3} Torr.

To verify the PLTR technique and the theoretical model developed in this work, a $25.4 \mu\text{m}$ thick Pt wire is measured first. During the experiments, two different pulse energies are used to heat the sample and record the experimental data. The experimental conditions are all listed in Table 1.

Both data analysis methods are used to determine the thermal diffusivity. By using the least squares fitting method, the thermal diffusivity based on the two sets of data is fitted to be 2.53×10^{-5} and $2.50 \times 10^{-5} \text{ m}^2\text{s}^{-1}$, respectively, close to the value in the literature of $2.51 \times 10^{-5} \text{ m}^2\text{s}^{-1}$ (at 300 K).¹⁴ The characteristic point method also gives close thermal diffusivity 2.47×10^{-5} and $2.56 \times 10^{-5} \text{ m}^2\text{s}^{-1}$, respectively. Figure 1 shows the fitting results for Data 1 using both data analysis methods. Sound agreement is observed between the fitting results and the experimental data for global data fitting.

To further understand the experiment, we take Data 1 of the Pt wire as an example to estimate the temperature rise after pulsed laser heating. Based on the measured voltage rise ΔV over the sample, the average temperature increase can be estimated using the equation $\Delta V/V = \varepsilon \Delta T$, where ε is the temperature coefficient of resistance for Pt and V is the voltage across the Pt wire when feeding the

current I (before laser heating). In the experiment, ΔV is 1.795 mV and V is 29.12 mV. Taking ε as $3.927 \times 10^{-3} \text{ K}^{-1}$,¹⁵ the overall average temperature increase is calculated to be 15.7°C . In order to have sound signals in the PLTR technique, a temperature increase of tens of degrees is required. For this level of temperature increase, the R - T relation for most metals can be treated as linear with sound accuracy. For example, Pt has a constant temperature coefficient of resistance ($3.927 \times 10^{-3} \text{ K}^{-1}$) within the temperature range of 0 – 100°C .¹⁵ The non-linear feature in the R - T relation will induce some second-order negligible uncertainty in final data processing.

3.2. Measurement of multi-wall carbon nanotube bundles

In this section, two types of MWCNT bundles, fabricated at the Oak Bridge National Laboratory, are measured. Scanning electron microscopy (SEM) study of the samples shows that there are MWCNTs with diameters from 30 to 50 nm inside the bundle. The alignment of the MWCNTs does not follow the axial direction of the bundle as shown in Fig. 2 (type 2 MWCNT).

The typical diameters of the MWCNT bundles are $200 \mu\text{m}$ and $30 \mu\text{m}$ for type 1 and type 2, respectively. Since the diameter of the type 1 MWCNT bundle is too thick, it will take a relatively long time to make the temperature uniform in the cross-section of the bundle after pulsed laser heating of one side of the bundle. As a result, the heat transfer will become two-dimensional. To measure the type 1 MWCNT bundle, a thinner bundle ($\sim 20 \mu\text{m}$) is peeled off it to conduct the measurement.

In the experiment, the MWCNT bundles are connected between two copper electrodes using

Table 1. Details of experimental conditions for the Pt wire.

	Data 1	Data 2
Length (mm)	3.513	
Diameter (μm)	25.4	
Resistance at room temperature (Ω)	0.791	
DC current (mA)	30	
Voltage of the wire when feeding the current (mV)	29.12	29.01
Voltage increase by laser pulse heating (mV)	1.795	1.026
Thermal diffusivity characteristic point ($10^{-5} \text{ m}^2\text{s}^{-1}$)	2.47	2.56
Thermal diffusivity least squares fitting ($10^{-5} \text{ m}^2\text{s}^{-1}$)	2.53	2.50

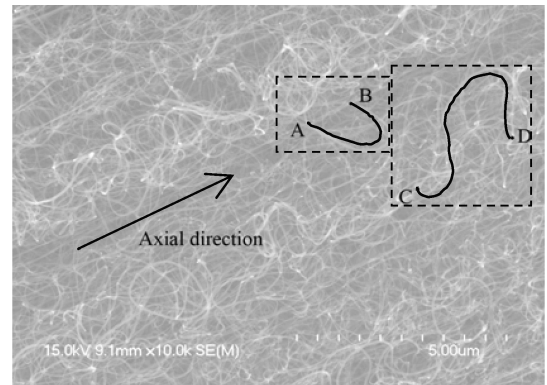


Fig. 2. SEM picture showing the CNT alignment inside the type 2 MWCNT bundle.

silver paste as shown in Fig. 3. Table 2 shows the length, resistance and other parameters of the MWCNT bundles measured in the experiment. When conducting experiments, it is observed that the temperature coefficient of resistance for the MWCNT bundles is negative, just like graphite

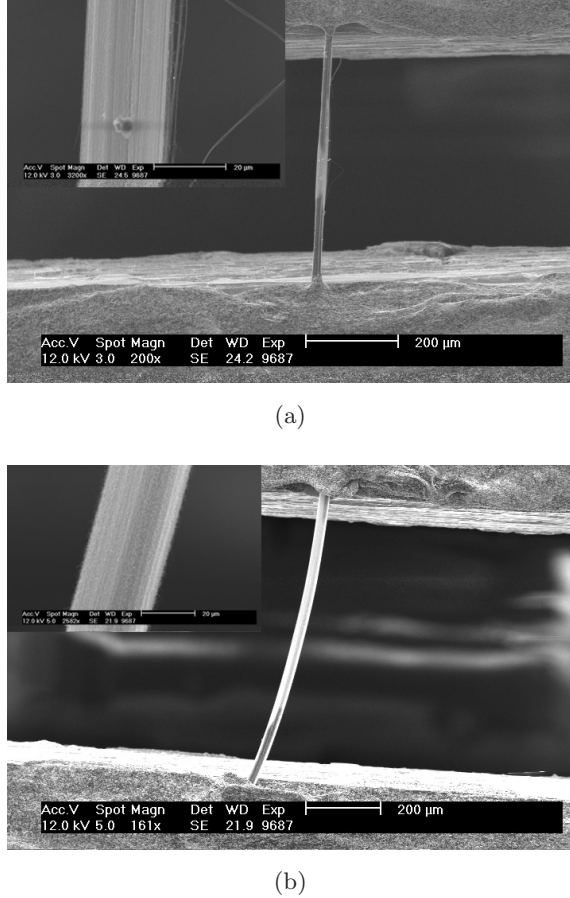


Fig. 3. SEM pictures of the two types of MWCNT bundles [(a) for type 1 and (b) for type 2] measured in the experiment.

Table 2. Details of experimental conditions and results for MWCNT bundles.

	Data 1	Data 2
Length (μm)	566.4	800.9
Diameter (μm)	23.3	29.7
DC current (mA)	0.2	0.1
Voltage of the wire when feeding the current (mV)	53.5	57.2
Voltage increase by laser pulse heating (mV)	-0.96	-1.07
Thermal diffusivity characteristic point ($10^{-5} \text{ m}^2 \text{ s}^{-1}$)	1.09	1.42
Thermal diffusivity least squares fitting ($10^{-5} \text{ m}^2 \text{ s}^{-1}$)	1.05	1.50

fibers. For the first type of bundle, the thermal diffusivity is fitted to be 1.09×10^{-5} and $1.05 \times 10^{-5} \text{ m}^2/\text{s}$ using the characteristic point and least squares fitting methods, respectively. For the second type of bundle, the fitted thermal diffusivity is 1.42×10^{-5} and $1.50 \times 10^{-5} \text{ m}^2/\text{s}$ by using the two methods. The sample is measured several times to check the repeatability of the technique. A measurement uncertainty of about 6.5% is observed. In order to check the reliability of measured thermal diffusivity for the two types of MWCNT bundles, the TET technique is used to measure the thermal diffusivity as well. For the type 1 MWCNT bundle, the TET measurement is conducted at the same time as the PLTR technique and the measured average thermal diffusivity is $1.05 \times 10^{-5} \text{ m}^2/\text{s}$, which further verifies the reliability of the PLTR technique and the thermal diffusivity obtained from the PLTR technique. The average thermal diffusivity measured using the TET technique for the type 2 MWCNT bundle is $1.18 \times 10^{-5} \text{ m}^2/\text{s}$, which is conducted one day after PLTR measurement and is slightly smaller than the value obtained from the PLTR technique. This is probably due to the extra vacuum pumping which leads to slight structural change, like the CNTs breaking inside. Furthermore, the TET technique is employed again to measure the intact (unpeeled) type 1 MWCNT bundle with a diameter around $200 \mu\text{m}$. The measured thermal diffusivity is $2.78 \times 10^{-5} \text{ m}^2/\text{s}$, which is more than twice the thermal diffusivity of the peeled bundle. Through this measurement, we can see that the peeling process can ruin the inside structure of the bundle.

The random alignment of CNTs in the bundle has a significant contribution to the measured low thermal diffusivity. Based on the alignment shown in Fig. 2, some first order estimation can be conducted to evaluate the real thermal diffusivity of single MWCNTs. Two typical MWCNTs are picked and analyzed. One is between point A and B as shown in Fig. 2. The length between A and B is $1.125 \mu\text{m}$ in the axial direction. But the real length of the MWCNT from A to B is $3.542 \mu\text{m}$, shown by the black curve in the figure. As the thermal diffusivity (α) is proportional to the square of length (L^2) in data processing, the thermal diffusivity of this single MWCNT is estimated to be $1.45 \times 10^{-4} \text{ m}^2/\text{s}$, which is about ten times the thermal diffusivity of the MWCNT bundle ($1.46 \times 10^{-5} \text{ m}^2/\text{s}$ for type 2). Similarly, taking the MWCNT between C and D for analysis, the direct length between C and D is $2.583 \mu\text{m}$ while

the MWCNT measures about $6.389\ \mu\text{m}$ from C to D. The thermal diffusivity of this single MWCNT is estimated to be $8.93 \times 10^{-5}\ \text{m}^2/\text{s}$. For more curved CNTs (many are shown in Fig. 2), their thermal diffusivities will be much larger than $8.93 \times 10^{-5}\ \text{m}^2/\text{s}$. Our estimation concludes that the real thermal diffusivity of MWCNTs should be about ten times the measured value. Considering the effect of the thermal contact resistance between CNTs, the real thermal diffusivity of single MWCNTs could be even higher.

The thermal diffusivity of MWCNTs obtained in this paper is at the temperature level of 10–20 degrees above the ambient temperature (298 K). According to work done by Fujii *et al.*,¹⁶ the thermal conductivity of CNTs in this temperature range has a weak dependence on temperature. While this paper focusses on the development of a novel technique for thermal characterization of micro/nanoscale wires/tubes, the next step in our research will be to investigate the temperature dependence of thermal diffusivity of MWCNT bundles within a large temperature range. Such knowledge will be critical for thermal design of functional materials in thermally hostile environments.

4. Conclusion

In this paper, a fast transient technique was developed to characterize the thermophysical properties of microscale wires/tubes. Two methods were developed for data analysis to obtain the thermal diffusivity of the sample. Employing this technique, the thermal diffusivity of Pt wires was measured. The measured results agreed well with the reference value. Our uncertainty analysis showed the experiment had an uncertainty better than 10%. The thermal diffusivity of MWCNT bundles was measured and the average value was 1.07×10^{-5} and

$1.46 \times 10^{-5}\ \text{m}^2/\text{s}$ for type 1 and type 2, respectively. The real thermal diffusivity of individual MWCNTs based on alignment analysis was estimated around $1.18 \times 10^{-4}\ \text{m}^2/\text{s}$.

Acknowledgments

Support for this work from the start-up fund of Iowa State University is gratefully acknowledged. The authors are grateful to Biqing Sheng, Dr. Zhaoyan Zhang, Kejun Yi, and Dr. Yongfeng Lu at the University of Nebraska-Lincoln for their help with using their high-power nanosecond pulsed lasers.

References

1. L. Lu, W. Yi and D. L. Zhang, *Rev. Sci. Instrum.* **72**, 2996 (2001).
2. T. Y. Choi *et al.*, *Nano Lett.* **6**, 1589 (2006).
3. J. Hou *et al.*, *J. Appl. Phys.* **100**, 124314 (2006).
4. P. Kim *et al.*, *Phys. Rev. Lett.* **87**, 215502 (2001).
5. L. Shi *et al.*, *Appl. Phys. Lett.* **84**, 2638 (2004).
6. G. Zhang and B. Li, *J. Chem. Phys.* **123**, 014705 (2005).
7. L. Benedict, S. Louie and M. Cohen, *Solid State Commun.* **100**, 177 (1996).
8. J. Hou, X. Wang and J. Guo, *J. Phys. D: Appl. Phys.* **39**, 3362 (2006).
9. J. Hou *et al.*, *Appl. Phys. Lett.* **88**, 181910 (2006).
10. J. Hou, X. Wang and L. Zhang, *Appl. Phys. Lett.* **89**, 152504 (2006).
11. J. Guo, X. Wang and T. Wang, *J. Appl. Phys.* **101**, 063537 (2007).
12. J. Guo *et al.*, *Appl. Phys. A* **89**, 153 (2007).
13. T. Wang *et al.*, *Appl. Phys. A* **87**, 599 (2007).
14. F. Incropera and D. Dewitt, *Fundamentals of Heat and Mass Transfer*, 5th Edn. (John Wiley & Sons Inc., New York, 2002), Appendix A.
15. R. Weast, *Handbook of Chemistry and Physics*, 64th Edn. (CRC Press Inc., Florida, 1983–84), pp. F-125.
16. M. Fujii *et al.*, *Phys. Rev. Lett.* **95**, 065502 (2005).